

Mechanical factors in primary water stress corrosion cracking of cold-worked stainless steel



Rashid Al Hammadi^a, Yongsun Yi^{b,*}, Wael Zaki^c, Pyungyeon Cho^b, Changheui Jang^d

^a Nuclear Security Division, Federal Authority for Nuclear Regulation, Abu Dhabi, United Arab Emirates

^b Department of Nuclear Engineering, Khalifa University, Abu Dhabi, United Arab Emirates

^c Department of Mechanical Engineering, Khalifa University, Abu Dhabi, United Arab Emirates

^d Nuclear and Quantum Engineering Department, Korea Advanced Institute of Science and Technology, Daejeon, South Korea

HIGHLIGHTS

- PWSCC of cold-worked austenitic stainless steel was studied.
- Finite element analysis was performed on a compact tension specimen.
- Mechanical fields near a crack tip were evaluated using FEA.
- The dependence of mechanical factors on K_I and yield stress was investigated.
- The crack tip normal stress was identified as a main factor controlling PWSCC.

ARTICLE INFO

Article history:

Received 12 November 2015

Received in revised form 17 February 2016

Accepted 20 February 2016

Available online 14 March 2016

Classification:

B. Materials engineering

ABSTRACT

Finite element analysis was performed on a compact tension specimen to determine the stress and strain distributions near a crack tip. Based on the results, the crack tip strain rates by crack advance and creep rates near crack tip were estimated. By comparing the dependence of the mechanical factors on the stress intensity factor and yield stress with that of the SCC crack growth rates, it was tried to identify the main mechanical factor for the primary water stress corrosion cracking (PWSCC) of cold-worked austenitic stainless steels. The analysis results showed that the crack tip normal stress could be the main mechanical factor controlling the PWSCC, suggesting that the internal oxidation mechanism might be the most probable PWSCC mechanism of cold-worked austenitic stainless steels.

© 2016 Elsevier B.V. All rights reserved.

1. Introduction

Austenitic stainless steels (ASS) have been widely used for reactor vessel internals because of their corrosion resistance, toughness, ductility, strength, and fatigue characteristics in the primary water conditions of pressurized water reactors (IAEA, 1999). The operating experience of ASS indicates that they have shown good performance in the primary water (PW) conditions (Tice et al., 2009) while intergranular stress corrosion cracking (IGSCC) of ASS has been reported as a generic problem in oxygenated water (Roychowdhury et al., 2011). However, some cases of IGSCC were reported on cold-worked ASS in the primary water conditions and

cold-work was found as a possible cause of the IGSCC (Couvant et al., 2007; Raquet et al., 2007). Since then, many studies have been performed on cold-worked ASS in the primary water conditions to examine the effects of mechanical, electrochemical, and material factors on the IGSCC (Tice et al., 2009; Lu et al., 2009). It has been identified that the IGSCC crack growth rate (CGR) of ASS increases with the degree of cold-work and consequently with the yield stress (Gómez-Briceno et al., 2009). Also, there are clear similarities in the primary water stress corrosion cracking (PWSCC) phenomena between ASS and nickel base alloys such as Alloy 600. For example, in the PW conditions, both types of materials show lower susceptibility to the IGSCC in sensitized conditions (Tice et al., 2009). For this reason, it has been tried to explain the IGSCC phenomenon of cold-worked ASS using the SCC mechanisms proposed for the PWSCC of Ni-base alloys such as slip dissolution, internal oxidation, and creep damage model. But, it seems that no mechanisms have fully explained the observations about the IGSCC occurring on cold-worked ASS and Ni-base alloys. This lack of

* Corresponding author. Tel.: +971 567338652.

E-mail addresses: rashid.alhammadi@fanr.gov.ae

(R.A. Hammadi), yongsun.yi@kustar.ac.ae (Y. Yi), wael.zaki@kustar.ac.ae (W. Zaki), pyungyeon.cho@kustar.ac.ae (P. Cho), chjang@kaist.ac.kr (C. Jang).

understanding of the IGSCC mechanism of both alloys in the PW conditions is attributed to many factors involved in the PWSCC phenomena (Rebak and Szklarska-Smialowska, 1996).

Although clear correlations have been found between the SCC crack growth rates of ASS in the PW conditions and the stress intensity factor or the degree of cold-work, only a few results have been reported on the mechanical factors near/at a crack tip as a function of the degree of cold-work. Shoji et al. (2010) compared qualitatively crack tip strain values between yield stresses of 160 MPa and 500 MPa calculated by different crack tip strain field formulations. But their further analysis was only on the crack tip strain rates. Several different mechanical factors that govern the IGSCC kinetics are identified in the proposed PWSCC mechanisms. The SCC crack growth rate (CGR) in the slip dissolution model (Andresen and Ford, 1988) is mainly governed by the crack tip strain rate (CTSR) among the mechanical factors. Through an analysis using a Weibull distribution of PWSCC damages, Shah et al. (1992) proposed the tensile stress as one of the main factors determining the crack growth rate of PWSCC. Also, in the internal oxidation model, the local tensile stress at a crack tip plays a main role in crack advance (Herbelin et al., 2009). Since the mechanical stress and strain fields near/at a crack tip control the PWSCC, analyzing the main mechanical factor would be an important step in identifying the possible PWSCC mechanism of cold-worked ASS.

In this study the mechanical factors around a crack tip were evaluated to investigate their effects on the PWSCC of cold-worked ASS. Finite element analysis (FEA) on a compact tension specimen was performed to calculate the stress and strain fields near a crack tip as a function of stress intensity factor, K_I , and yield stress, σ_{ys} . Other mechanical factors near a crack tip were estimated based on the FEA results. Along with the main mechanical factors, the possible mechanisms for the PWSCC of cold-worked ASS are discussed.

2. Finite element model and analysis

The finite element analysis was performed using ABAQUS (Version 6.11) on a 1/2 in. compact tension (CT) specimen (ASTM E647-08) with a crack length (a) of 12.16 mm shown in Fig. 1. For finite element analysis the sample model was meshed with two zones having different mesh shapes and sizes as shown in Fig. 2. Theoretically, crack tip asymptotic fields have been expressed as a function of r that is a distance from the crack tip on the crack plane. According to Shoji et al. (2010) the characteristic distance r_0 where the mechanical factors for SCC are evaluated was estimated to have a micrometric level. Therefore, near the crack tip, the geometry model for a CT specimen was finely meshed as an element with $20 \mu\text{m} \times 20 \mu\text{m}$ size and square shape while the remaining portion of the model was meshed as randomized quadrangle shape. The element applied to the whole region of a CT specimen was 8-node biquadratic plane strain quadrilateral element, ABAQUS element CPE8, which has 8 nodes and fully 9 integration points as shown in Fig. 3.

The distributions of the stress and strain fields in the compact tension specimen were determined numerically by means of FEA. For this purpose, a finite element model was constructed to solve the boundary value problem representing the CT specimen containing a crack with traction-free lips.

The upper pin was modelled as a rigid body because of the usually very small strains experienced by the pin during proper tensile testing. The opening of the crack was obtained by subjecting the upper pin to an upward concentrated force F , with rigid and frictionless contact conditions defined at the interface between the pin and the hole.

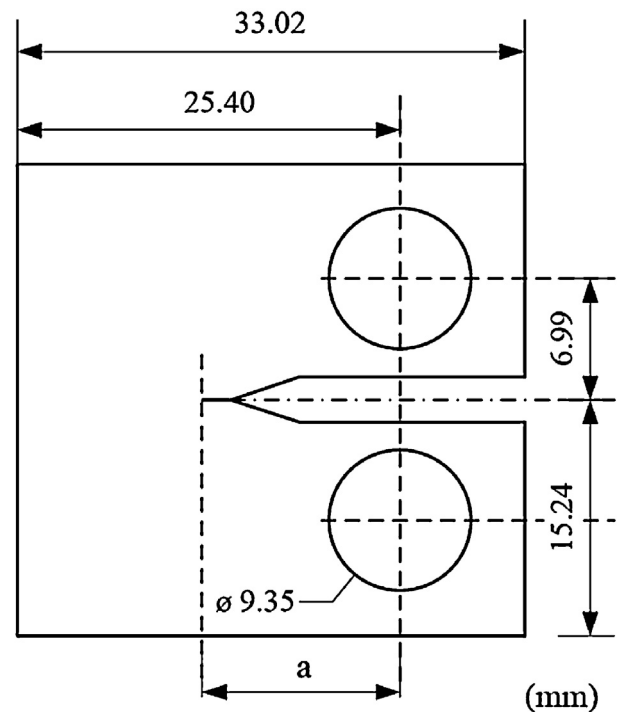


Fig. 1. Geometrical model of compact tension specimen.

The constitutive behaviour of the steel alloy was considered elastoplastic with isotropic hardening, for which the stress-strain relation is given by

$$\sigma = \mathbf{C} : (\boldsymbol{\varepsilon} - \boldsymbol{\varepsilon}^p) \quad (1)$$

where $\boldsymbol{\varepsilon}$ is the total strain, $\boldsymbol{\varepsilon}^p$ is the plastic strain and \mathbf{C} is the elastic stiffness tensor of the material, function of Young's modulus E and Poisson's ratio ν assuming isotropic stress-strain behaviour. The isotropic strain hardening beyond the onset of plastic deformation is determined from tensile stress vs. plastic strain data provided to the FEA software as user input. The time integration of the above equations is accomplished by means of FEA where the load defined by the upward force F acting on the upper pin is discretized into increments and the boundary value problem is solved iteratively for each load increment. This procedure gives access to the displacement field at the nodes of the mesh elements and to stress and strain fields at the integration points within.

The calculation results were compared with experimental SCC crack growth rates of 316 stainless steel measured by Terachi et al. (2012). Therefore, the material properties of 316 stainless steel available in literature were used. The stress-strain behaviour of 316 stainless steel was expressed by the Ramberg–Osgood equation (Xue et al., 2009):

$$\varepsilon = \frac{\sigma}{E} + \left[\alpha \times \left(\frac{\sigma_{ys}}{E} \right) \times \left(\frac{\sigma}{\sigma_{ys}} \right)^n \right] \quad (2)$$

where E is the Young's modulus, σ_{ys} is the yield strength, α is the dimensionless material constant, and n is the strain hardening exponent of the material. The input parameters used in this analysis are shown in Table 1.

3. Effect of mechanical factors on PWSCC

3.1. K_I and σ_{ys} dependence of SCC crack growth rates

By comparing the respective dependence of mechanical factors near a crack tip determined by the finite element analysis on K_I and

Download English Version:

<https://daneshyari.com/en/article/295945>

Download Persian Version:

<https://daneshyari.com/article/295945>

[Daneshyari.com](https://daneshyari.com)